A Lignin-containing Hemicellulose-based Hydrogel and its Adsorption Behavior

Xiyi Song, Fangeng Chen,* and Shangjun Liu

A lignin-containing hemicellulose-based hydrogel was prepared from acylated hemicellulose and acrylic acid by free radical polymerization reaction, initiated by ammonium persulfate and N,N,N',N'-tetramethyl-ethane-1,2-diamine in the presence of sodium lignosulfonate. Sodium lignosulfonate present in the hydrogel, when grafted by poly(acrylic acid), was identified as an interpenetrating polymer network form, while that not grafted by poly(acrylic acid) was identified as a semi-interpenetrating polymer network form. Both the swelling ratio and the adsorption capacity were dependent on sodium lignosulfonate dosage. The adsorption behavior of the hydrogel was evaluated. The maximum adsorption capacity towards methylene blue, a model dye, was 2691 mg/g. The adsorption kinetics and isotherm were well fitted by pseudo-second-order kinetics and Langmuir isotherm model, respectively. The hydrogel reveals an approximately 80% adsorption efficiency after fourth recycle. This hydrogel is a promising material for dye wastewater treatment.

Keywords: Hemicellulose; Sodium lignosulfonate; Hydrogel; Adsorption; Methylene blue

Contact information: State Key Laboratory of Pulping and Paper Engineering, South China University of Technology, No. 381, Wushan Road, Guangzhou, 510640, China;
** Corresponding author: fgchen@scut.edu.cn*

INTRODUCTION

Dyes are used in manufacturing various products. As a result of the wide application of dyes, the pollution from dye wastewater has become a worldwide environmental issue in the modern textile, printing, paper, and dyeing industries (Gupta *et al.* 2006). It is recognized that even very small amounts of dye in water can increase the chromaticity value. Simultaneously, the dye effluent is sometimes toxic, mutagenic, or carcinogenic to various microorganisms and aquatic animals. The pollutant can be dispersed throughout the entire food web, resulting in effects on the human body, such as tissue death, elevated heart rate, and other adverse impacts (Yi and Zhang 2008).

Various techniques, including physical, chemical and biological, have been developed for dye wastewater treatment (Feng *et al.* 2014). Among them, adsorption is an efficient method. Some natural polymers, *e.g.*, cellulose derivatives, have been reportedly used in wastewater treatment (Goel *et al*. 2015).

A hydrogel is a kind of highly hydrophilic material that is formed by polymer chains connected together in a three-dimensional network by physical or chemical interactions. Some hydrogels possessing ionic groups have been used for adsorbing ionic dyes in wastewater (Jing *et al.* 2012; Guo *et al.* 2015; Peng *et al.* 2015). Recently, special attention was paid to hydrogels prepared from hemicellulose (Peng *et al.* 2012; Dax *et al.* 2014), a heterogeneous polysaccharide, accounting for 15% to 35% in lignocellulosic feedstock. Hemicellulose can be modified at its hydroxyl groups to obtain various

derivatives (Dax *et al.* 2015). A temperature-sensitive hydrogel was prepared from hemicellulose derivatives and N-isopropylacrylamide (Yang *et al.* 2011).

Lignin, as the second most abundant natural polymer in the world, often appears as a by-product of pulping and has limited utilization as a fuel. Sodium lignosulfonate (NaLS), an important technical lignin product, contains hydrophilic sulfonate groups and hydrophobic phenyl propane matrix within its molecules. It is reported that the addition of lignin into hydroxypropyl cellulose-based hydrogel can decrease the lower critical solution temperature (LCST) of the hydrogel (Uraki *et al.* 2004). The introduction of lignin into a hydrogel can also reduce the LCST of PNIPAAm hydrogel (Feng *et al.* 2012). Therefore, lignin is expected to impact the properties of hemicellulose-based hydrogel when it is added to the hydrogel. However, to the best of our knowledge, the impact of lignin on the adsorption performances of the hydrogel has not been reported.

In this study, a hemicellulose-based hydrogel with various contents of NaLS was prepared and characterized. The hydrogel was synthesized by grafting acrylic acid from acylated hemicellulose (AHC) and the phenolic hydroxyl group of NaLS by free radical polymerization and subsequent crosslinking. The structures of hemicellulose, AHC, and the resulting hydrogels were characterized by Fourier transform infrared (FT-IR) and proton-nuclear magnetic resonance (^{1}H-NMR) technique. The existing forms of NaLS were investigated by ultraviolet spectrophotometry indirectly. The morphology and swelling properties were also investigated. Methylene blue (MB), a cationic dye, was used to investigate the adsorption and reusability properties of the hydrogel. As a model of dye, methylene blue is frequently used to investigate the adsorption of organic dyes from aqueous solution because it gathers in many active sites in organic dyes, *e.g.*, thiazine, phenyl, alkyl, and amino- groups, creating a wide range of prospective physical and/or chemical interactions between adsorbents and organic pollutants (Mekewi *et al.* 2015).

EXPERIMENTAL

Materials

Corn cob powder was obtained from Henan, China. Maleic anhydride (MA), lithium chloride (LiCl), anhydrous lithium hydroxide (LiOH), and sodium lignosulfonate (NaLS) were commercial products of Aladdin (Sigma-Aldrich Biotechnology Reagent Inc., China). Acrylic acid (AA) was a product of Tianjin Fuchen Chemical Reagents Factory, China. Ammonium persulfate (APS), N,N,N',N'-tetramethyl-ethane-1, 2-diamine (TEMDA), and methylene blue (MB) were products of Tianjin Kemiou Chemical Reagent Company, China. All reagents used were of analytical grade.

Isolation of Hemicellulose from Corn Cob

The powdered corn cob was passed through a 40-mesh sieve and then oven-dried at 105 °C for 3 h. The dried powder was extracted with benzene-ethanol mixture (2:1, v/v) for 6 h to remove wax and other extractives and then air-dried. The dewaxed corn cob was treated with 0.92% (w/v) $NaClO_2$ solution (pH = 4.0) at 75 °C for 3 h to finish the delignification and then dried to obtain holocellulose. Thereafter, the holocellulose was extracted with a 20-fold excess of 8% (w/v) KOH aqueous solution at room temperature for 16 h and then filtered. The filtrate was neutralized to pH 5.5 with acetic acid and then concentrated by rotary evaporation and precipitated in a triple volume of 95% ethanol. The precipitate was freeze-dried to obtain hemicellulose. The hemicellulose was pre-

hydrolyzed with 72% H_2SO_4 for 1 h at 30 °C and hydrolyzed with 3% H_2SO_4 for 2 h at 121°C. The neutral sugar composition of the hydrolysate solution was determined by ion chromatography. The hemicellulose contained 83.2% of xylose, 7.9% of glucose and 6.1% of arabinose (based on total sugar content). The hemicellulose was dissolved in deionized water at 90 °C and cooled to room temperature for gel permeation chromatography (GPC) analysis. The weight-average molecular weight and number-average molecular weight of hemicellulose were measured to be 47,000 and 33,000, respectively.

Preparation of Acylated Hemicellulose (AHC)

The acylated hemicellulose (AHC) was prepared from corn cob hemicellulose and maleic anhydride in the presence of anhydrous dimethylsulfoxide as the solvent and LiOH as the catalyst. The procedure was based on an earlier study (Yang *et al.* 2011) with minor modifications. To a 100-mL three necked round-bottomed flask equipped with a dry nitrogen gas inlet, 0.3 g of LiCl and 1 g of hemicellulose were added, followed by 20 mL of anhydrous DMSO. The mixture were placed at 80 °C for 0.5 h. Subsequently, anhydrous LiOH was added to the flask and stirred for 15 min. Maleic anhydride (0.5 g) dissolved in 5 mL of anhydrous dimethylsulfoxide was added to the flask drop-wise. The mixture was heated to 80 °C for 2 h and then precipitated in a four-fold excess (by volume) of 95% ethanol and washed with 80% ethanol thoroughly. The AHC product was freeze-dried under vacuum at -50 °C for 24 h.

The degree of substitution (DS) of AHC is the average number of hydroxyl groups being substituted per xylose unit. The maximum possible DS of the corn cob hemicellulose is 2.0, corresponding to the number of hydroxyls available on the backbone of the xylose unit. The DS of AHC was estimated by ^{1}H-NMR (Bruker DRX-400, USA) using D_2O as the solvent (Belmokaddem *et al.* 2011). The DS was calculated by the ratio of the area of double bond proton resonance signal (appearing at 5.8 ppm and 6.6 ppm) to that of the anomeric proton in the pyran ring of xylan at 4.4 ppm.

Hydrogel Preparation

Acylated hemicellulose (0.3 g) and various amounts of NaLS (0 g, 0.05 g, 0.1 g, 0.15 g and 0.2 g, labeled as Gel-1 through Gel-5) were dissolved in 3 mL of deionized water in a flat-bottom glass tube at 50 °C. After being bubbled with N_2 to remove oxygen, 0.1 g of APS and 0.1 mL of TEMDA were added to the solution, and the solution was stirred for 1 min. Then, 3.0 g of acrylic acid was added. The stirring was stopped when the viscosity of the mixture increased. The tube was sealed with a rubber plug and was placed in a water bath at 50 °C for 3 h to form the hydrogel.

The hydrogel was collected and cut into uniform pieces. The pieces were immersed in deionized water at room temperature for three days to remove unreacted chemicals. Deionized water was changed every 6 h. The hydrogels obtained were freeze-dried at -50 °C for 24 h.

FT-IR and ^{1}H-NMR Analysis

The FT-IR spectra of hemicellulose, AHC, and dried hydrogel were recorded on a Bruker Vector 33 apparatus. The samples were dried and milled into powder. Then FT-IR analysis were conducted by KBr pellet method within the wave number range of 4000 to 400 cm^{-1}. The ^{1}H-NMR spectra of hemicellulose and AHC were recorded on a Brucker-400MHE NMR spectrometer (Bruker, Germany) using D_2O as the solvent.

Morphological Analysis

The interior morphology of the hydrogel was observed with a scanning electron microscope (Carl Zeiss Jena GmbH-EVO 18, Germany). The swollen or adsorbed hydrogel samples were freeze-dried and then sputter-coated with a layer of gold with a sputter coater (Beijing Elaborate Technology Development Ltd., ETD-2000, China)

Investigation of the Existence of NaLS

The forms of NaLS present in the hydrogels were investigated, since they may have an influence on the interior morphology as well as the swelling properties and adsorption capacity of the hydrogels. Two groups of dried hydrogels (Gel-1 to Gel-4) were used. One group was thoroughly extracted by deionized water at 90 °C and the solid residue was collected for FT-IR characterization, while the extraction solution was used for the ultraviolet spectrophotometry test. The other group was dissolved in 1 M sodium hydroxide solution (0.15%, w/v) for 24 h to obtain the solution for ultraviolet spectroscopic analysis. The UV absorbance of the two groups of solution was measured at 280 nm by ultraviolet spectrophotometry (Scinco S3100, South Korea). Gel-1, which contained no NaLS, was used for the background correction.

The NaLS in the hydrogel is expected to exist in three forms: (1) dissociated form, which is blended in hydrogel, can be extracted by deionized water at room temperature in three days; (2) semi-interpenetrating polymer network (semi-IPN), which is extracted in deionized water at 90 °C in 3 h, is combined with the hydrogel by physical interaction; and (3) interpenetrating polymer network (IPN), which endures the process of elution and extraction, is grafted by acrylic acid by chemical bonding. To confirm the content of NaLS, calibration curves of NaLS in deionized water and in 1 M sodium hydroxide solution were established by the absorbance of lignin as a function of lignin concentration. The content of the three parts of NaLS was calculated by Eqs. 1 to 4,

$$w_{\text{semiIPN}} = (C_1 \times V_1)/m_1 \quad (1)$$

$$w_{\text{IPN}} = (C_2 \times V_2)/m_2 - w_{\text{semiIPN}} \quad (2)$$

$$w_{\text{i}} = m_{\text{NaLS}}/(m_{\text{NaLS}} + m_{\text{AA}} + m_{\text{AHC}}) \quad (3)$$

$$w_{\text{free}} = w_{\text{i}} - w_{\text{semiIPN}} - w_{\text{IPN}} \quad (4)$$

where w_{semiIPN}, w_{IPN}, w_{free}, and w_{i} represent the contents of NaLS (mg/g) in semi-IPN, IPN, free state, and the initial added NaLS, respectively; C_1(mg/mL) and C_2(mg/mL) are the concentration of NaLS in extracted deionized water and in 1 M sodium hydroxide solution, calculated from the corresponding calibration curve, respectively; V_1(mL) and V_2(mL) are the volume of the deionized water and 1 M sodium hydroxide solution, respectively; m_1(g) and m_2(g) are the weights of dry hydrogel added to the extracted deionized water and 1 M sodium hydroxide solution, respectively; and m_{NaLS} (g), m_{AA} (g), and m_{AHC} (g) are the weights of NaLS, AA, and AHC.

Swelling Behaviors of Hydrogels

The swelling ratio (*SR*) of the hydrogels was studied by gravimetric method in deionized water (pH = 6.8) at room temperature. The *SR* was obtained by weighing each sample at a given time after the excess surface water was carefully wiped off with moistened filter paper. The data were measured in triplicate and the average value is reported. The *SR* was calculated according to Eq. 5,

$$SR = (m_t - m_0)/m_0 \quad (5)$$

where m_t and m_0 are the weights (g) of the swollen and dried hydrogel, respectively.

Adsorption Kinetics and Equilibrium Adsorption Isotherm

For adsorption kinetics, approximately 50 mg of dried hydrogel (Gel-1 through Gel-4) was immersed in 200 mL MB solution (200 mg/L) at 30 °C and then placed in an oscillating machine with a constant rate of 100 rpm for different periods (in hours). The influence of temperature on the equilibrium adsorption was investigated with Gel-3. The adsorption experiment lasted for 24 h in 200 mL MB solution (200 mg/L) at 30 to 70 °C, and the amount of adsorption was calculated. For the equilibrium adsorption isotherm, 50 mg of dried hydrogel was immersed into 100 mL of MB solution (concentration 50 to 1000 mg/L) for 24 h. The ionic strength of MB solution was adjusted to 0.01 M with NaCl, and the pH was adjusted to 10.0 with 0.01 M NaOH solution. To determine the MB concentration, 2 mL of MB solution was taken from the adsorption system and was measured using an ultraviolet spectrophotometer at 664 nm. Each sample was tested three times, and the adsorption capacity was calculated from the average data. The adsorption amount of MB at time t (Q_t) and the ratio of removal (R_r) were calculated by Eqs. 6 and 7,

$$Q_t = (C_0 - C_t) \times V/m \quad (6)$$

$$R_r = (C_0 - C_t)/C_0 \quad (7)$$

where C_0 and C_t represent the MB concentration at the initial time and time t (mg/L), respectively, V is the volume of MB solution (mL), and m is the weight of the dried hydrogel (g).

Reusability Performance of Hydrogel

Approximately 50 mg dry hydrogel (Gel-3) was added to 200 mL MB solution (200 mg/L, pH=10) for 12 h to reach its adsorption equilibrium. The MB-loaded hydrogel was filtered by 400-mesh gauze, and washed with deionized water. Thereafter, the MB-loaded hydrogel was immersed in 200 mL HNO_3 solution (0.1 M) for 2 h to regenerate, and then was collected from the HNO_3 solution, and washed with distilled water. The recovered hydrogel was reused in the next cycle of adsorption experiment. The adsorption-desorption experiment was conducted for five cycles. The adsorption capacity of the hydrogel was calculated according to Eq. 6. The recycle efficiency (R %) of regenerated hydrogel was calculated according to Eq. 8,

$$R\,\% = Q_n/Q_1 \times 100\% \quad (8)$$

where Q_n is the adsorption capacity of the hydrogel in the nth cycle, Q_1 is the adsorption capacity of the hydrogel in the first cycle.

RESULTS AND DISCUSSION

Preparation of AHC and Hydrogels

In this work, acylated hemicellulose (AHC) was prepared from corn cob hemicellulose and maleic anhydride. Subsequently, AHC was used to react with acrylic acid to yield hydrogels. Figure 1 shows the ^{1}H-NMR spectra of the original hemicellulose and AHC. The newly appeared signals at 5.8 and 6.6 ppm were assigned to the protons of

-CH=CH- (Hamcerencu *et al.* 2008). The signals appearing at 3.0 to 4.5 ppm were attributed to the protons of the pyran ring of xylan, while the signal at 4.4 ppm was assigned to the anomeric proton of the pyran ring of xylan (Fundador *et al.* 2012). The degree of substitution (DS) of AHC was calculated to be 0.42 based on Eq. 1, indicating a successful grafting reaction between hemicellulose and maleic anhydride.

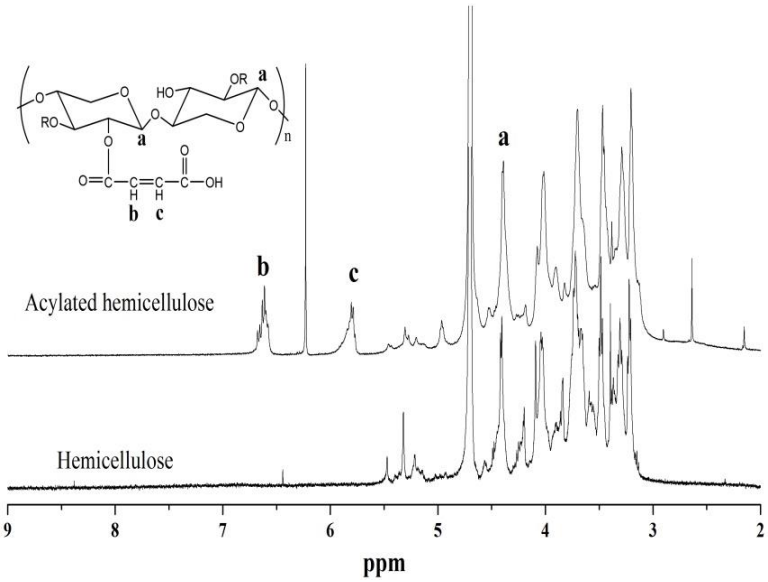

Fig. 1. ^{1}H-NMR of hemicelluloses and acylated hemicellulose derivative

During the reaction between acrylic acid and AHC (or NaLS), acrylic acid was grafted to both -CH=CH- of AHC or phenolic hydroxyls of NaLS. The hydrogel was synthesized by the crosslinking between the structural units. In this study, Gel-5 collapsed in deionized water, so that it was not studied in the following experiments.

FT-IR Spectra

Figure 2 shows the FT-IR spectra of NaLS, hemicellulose (HC), AHC, and Gel-3 extracted by water.

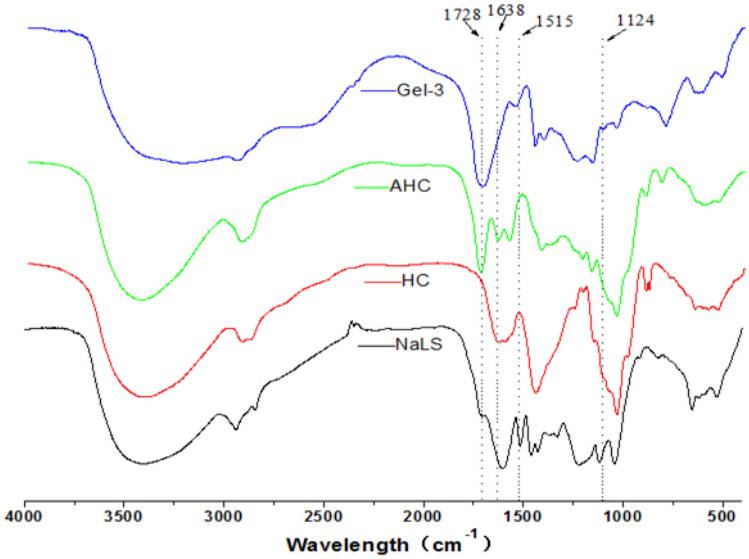

Fig. 2. FT-IR spectra of NaLS, HC, AHC, and extracted Gel-3

The bands at 1728 cm^{-1} and 1638 cm^{-1}, representing carbonyl group and -C=C- double bond in AHC, respectively, illustrate that maleic anhydride was successfully grafted to hemicellulose (Hamcerencu *et al.* 2008). The band at 1638 cm^{-1} does not appear within Gel-3 indicating that -C=C- double bond in AHC is converted to single bond during graft copolymerization. The band at 1724 cm^{-1} representing carbonyls is broadened by the introduction of acrylic acid. The peaks of aromatic rings at 1515 cm^{-1} and sulfonate at 1124 cm^{-1} still appear in the extracted Gel-3, indicating the existence of NaLS in Gel-3.

The Existence States of NaLS

The contents of lignin in different states are listed in Table 1. NaLS in dissociated state can be soaked out by deionized cool water, suggesting that this part of NaLS did not combine with the hydrogel network by physical or chemical ways. The portion of NaLS that was extracted from the hydrogel by deionized hot water (90 °C) can be thought to have been in semi-IPN form. Gel-4 contained a relatively high content of semi-IPN NaLS, which illustrates that the increase in addition of NaLS resulted in more NaLS in semi-IPN form. Moreover, too much NaLS in the initial mixture seems not conducive to the formation of hydrogel. Some portion of NaLS could not be extracted in deionized water at 90°C, which was thought to be in IPN form. This part of NaLS was probably grafted by acrylic acid from the phenolic hydroxyl position (Ouyang *et al.* 2006). Gel-3 has a high content of NaLS in IPN form resulting in compact pores that favors the adsorption capacity.

Table 1. The States of NaLS in Dried Hydrogels

Existence form of NaLS (mg/g)[a]	Gel-1	Gel-2	Gel-3	Gel-4
Initial added	0	14.93	29.41	43.48
Free state	0	4.05	4.35	10.05
semi-IPN form	0	5.72	6.11	29.73
IPN form	0	5.16	18.95	3.70
[a] mg of NaLS per gram of reagents used in its formulation (AA+AHC+NaLS)				

SEM Characterization

Figure 3 shows the interior morphology of the hydrogels with different contents of NaLS. The hydrogels present honeycomb-like structures, favoring water penetration to the hydrogels' matrix. However, with the increase in NaLS/AHC mass ratio, the pore size of the hydrogels did not show notable change. This result may be explained by the low content of NaLS in the hydrogel. For example, Gel-1 was NaLS free, while Gel-4 with largest amount of NaLS was approximately 4.4% (w/w). Gel-3 showed a slight narrow pore which was probably caused by the high content of IPN form NaLS (Table 1). Meanwhile, NaLS is considered a surface-active substance and has a strong hydrophilic effect, demonstrating good physical interaction with the poly(acrylic acid) chain and resulting in a small effect on the pore size of the polymer matrix.

Swelling Properties of Hydrogels

The effects of NaLS/AHC mass ratio on the swelling capacities of the hydrogels in deionized water are shown in Fig. 4. The results reveal that the hydrogels presented a high water uptake rate in the initial 10 h and a slow water uptake rate after that. The hydrophilic hydrogel network creates osmotic pressure, which causes the water uptake process. With the dissociation of the –COOH groups, the charge density increases, resulting in the enhancement of the osmotic pressure inside the hydrogel.

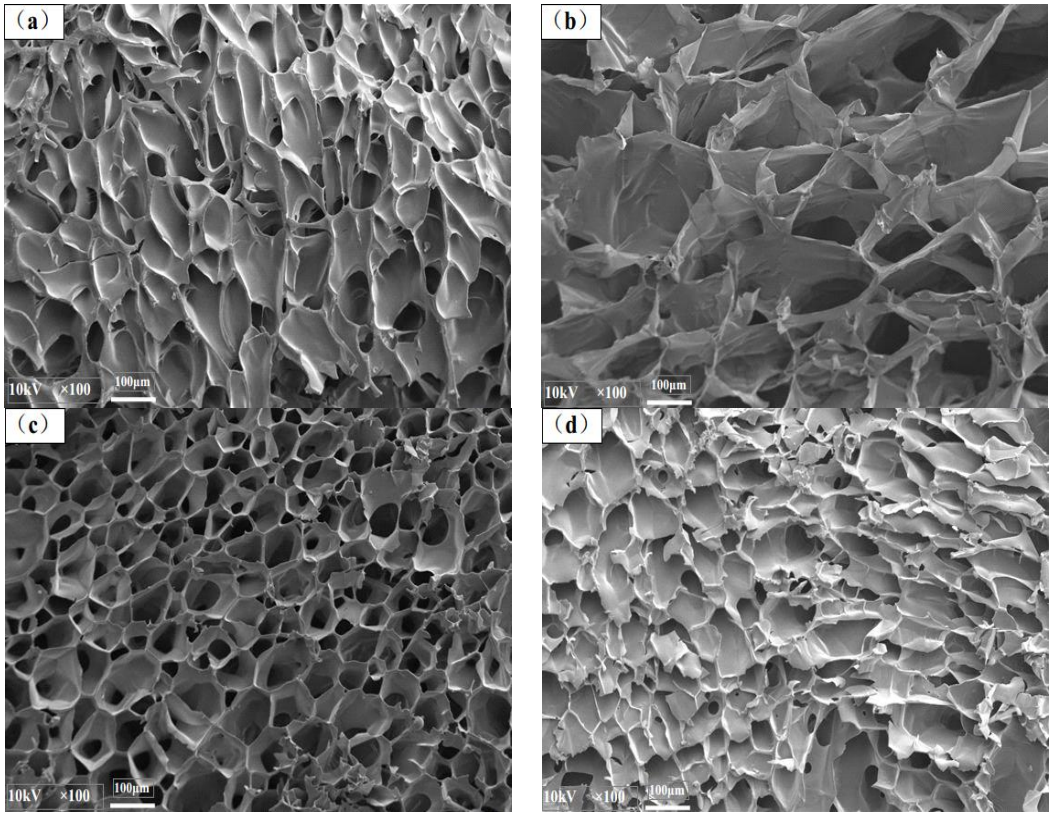

Fig. 3. SEM images of Gel-1 (a), Gel-2 (b), Gel-3 (c), and Gel-4 (d)

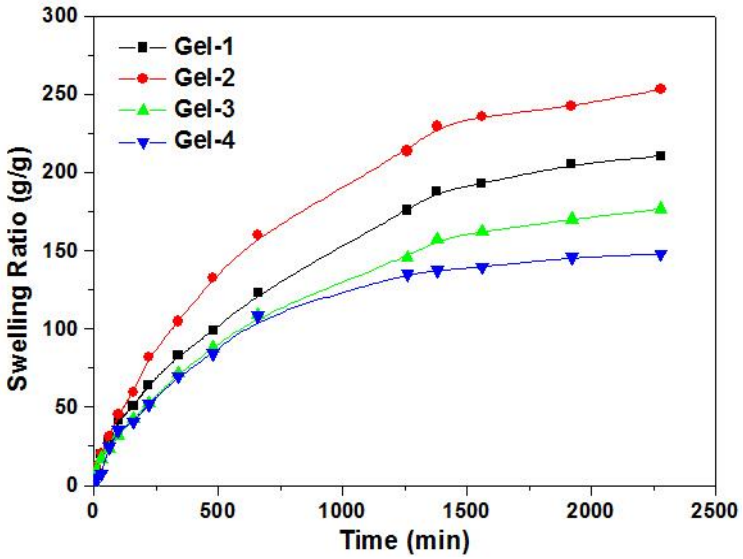

Fig. 4. The impact of time on the swelling ratio of the hydrogels

The osmotic pressure difference between the internal and external solution of the network is balanced by the swelling of the gel (Mahdavinia *et al.* 2004). The maximum *SR* increases from 210 to 253 g/g as the NaLS/AHC mass ratio increases from 0 to 1/6. However, the equilibrium *SR* decreases from 253 to 148 g/g with an increase in the NaLS/AHC mass ratio from 1/6 to 1/2. This result may be attributed to the decreased

surface tension of the absorbed water because of the additive NaLS, which is regarded as a kind of surface active material. Conversely, the rigid phenyl propane unit of NaLS penetrating the soft poly-acrylic acid chains possibly increases the firmness of the hydrogels, resulting in a decrease in *SR*.

Effect of Contact Time on Adsorption

Methylene blue (MB) was used to investigate the adsorption kinetics of the hydrogels. Based on the negatively charged poly(acrylic acid) hydrogel and the cationic dye MB, the electrostatic attraction between negatively charged hydrogel and positively charged MB can describe the main adsorption process (Liu *et al.* 2011).

As shown in Fig. 5, the adsorption amount increased sharply in the initial 2 h, and the adsorption rate was in the range of 50 to 150 mg/(g·h). The adsorption rate decreased below 50 mg/(g·h) in the period 2 to 8 h. The adsorption equilibrium was achieved in 8 h. The adsorption amount increased from 328 to 362 mg/g when the NaLS/AHC mass ratio increased from 0 to 1/3. This result is attributed to the fact that the addition of NaLS, which introduces RSO_3^- into the hydrogel matrix, facilitates adsorption. Meanwhile, an increase of IPN form of NaLS (Table 1) may contribute to the high adsorption capacity. However, the adsorption capacity decreased from 362 to 297 mg/g when the NaLS/AHC mass ratio increased from 1/3 to 1/2. This result may be attributed to the rigid phenyl propane units of NaLS, which enhance the rigidity of the polymer network and reduce the *SR*, and the adsorption capacity was thus reduced.

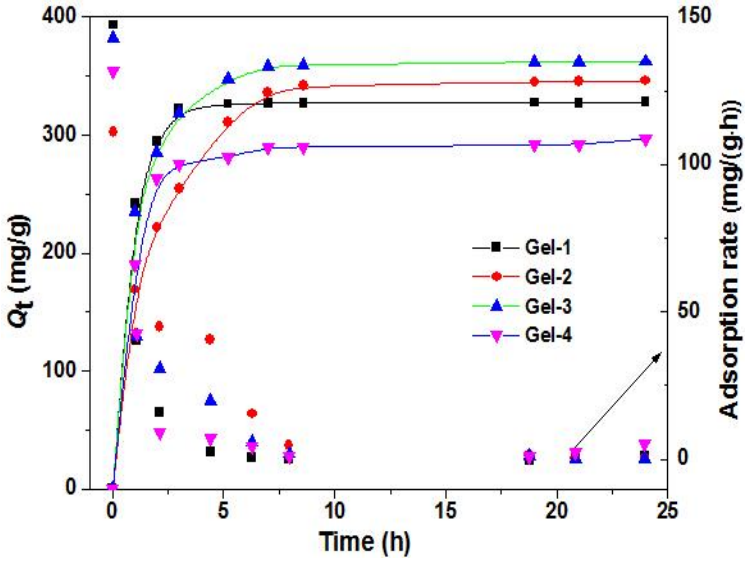

Fig. 5. Impact of time on the adsorption amount of hydrogels

The pseudo-first-order kinetics and pseudo-second order kinetics are two frequently used models to study the adsorption mechanism. The equations are given as Eq. 9 and Eq. 10 (Kannan and Sundaram 2001), respectively,

$$\frac{1}{Q_t} = \frac{K_1}{Q_m t} + \frac{1}{Q_e} \quad (9)$$

$$\frac{t}{Q_t} = \frac{1}{k_2 Q_c^2} + \frac{t}{Q_c} \quad (10)$$

where Q_t (mg/g) is the amount of MB absorbed at time t; Q_e (mg/g) is the amount of MB absorbed at adsorption equilibrium time; and K_1 (min^{-1}) and K_2 ($g/h^{-1}\cdot mg^{-1}$) are the rate constants of pseudo-first-order and pseudo-second-order kinetics models, respectively. The fitting results are listed in Table 2. Notably, the coefficients of determination for the pseudo-second- order model (R_2^2) were larger than those of the pseudo-first-order model (R_1^2), and the adsorption capacities ($Q_{e(cal)}$) calculated by the pseudo-second-order kinetics model were generally close to the theoretical adsorption capacity ($Q_{e(exp)}$), which suggests that the adsorption system could be well fitted by the pseudo-second-order kinetics model.

Table 2. Parameters of Adsorption Kinetics of MB onto Hydrogels

Sample	$Q_{e(exp)}$[a]	Pseudo-first-order kinetics model			Pseudo-second-order kinetics model		
		K_1(min^{-1})	$Q_{e(cal)}$[b]	R_1^2	K_2($g/h^{-1}\cdot mg^{-1}$)	$Q_{e(cal)}$[b]	R_2^2
Gel-1	327	0.3630	342	0.9143	0.02341	330	0.9998
Gel-2	345	1.1454	373	0.9831	0.003655	358	0.9979
Gel-3	362	0.5864	379	0.9870	0.008017	368	0.9996
Gel-4	296	0.5417	310	0.9072	0.01280	298	0.9996

[a] The equilibrium adsorption capacity detected by experiments
[b] The theoretical equilibrium adsorption capacities calculated by the two models

Effect of Temperature and Initial Concentration on Adsorption

Figure 6 shows that the temperature had a negative effect on the adsorption capacity of Gel-3 in the range 30 to 70 °C.

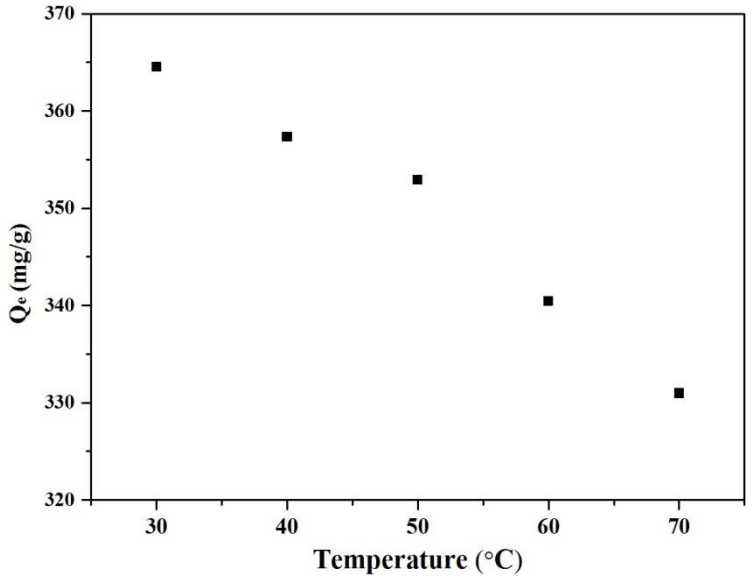

Fig. 6. Impact of temperature of MB solution on *Q*e of Gel-3

The results in Fig. 6 are similar to those reported in literature. (Liu *et al* 2011). As a cationic dye, MB presents an adsorption behavior similar to Cr (VI) and Ni (II) ions as

reported. According to Kumar *et al.* (2009), the decrease in adsorption of Zn (II) ions with the rise in temperature may be due to either damage of active binding sites in biomass or increasing tendency to desorb metal ions from the interface to the solution. The results in Fig. 6 can also be explained by same reason.

The impact of the initial concentration of MB on the Q_e of hydrogels was studied, and the results are depicted in Fig. 7. The adsorption ability increased with increasing initial concentration of MB and exhibited an adsorption plateau when the concentration of MB is 2400 mg/L. However, the removal ratio decreased with increasing MB concentration. This result may be due to an inadequate number of adsorption sites as well as competitive adsorption of MB (Zhao *et al.* 2012). Interestingly, the additive NaLS contributes positively to the adsorption ability, *e.g.*, Gel-3, with a NaLS/AHC mass ratio of 1/3, has the maximum adsorption capacity; this result corresponds with the adsorption kinetics experiment.

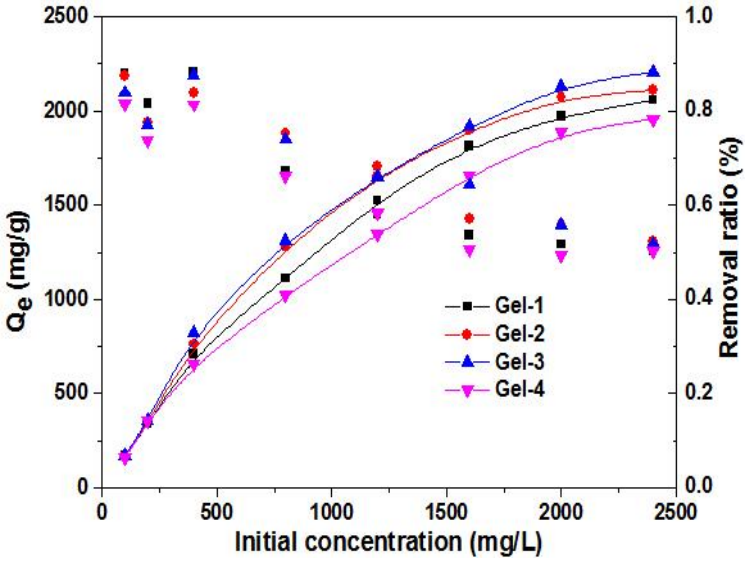

Fig. 7. Impact of initial concentration of MB on *Q*e of the hydrogels

Langmuir isotherms and Freundlich isotherms are often adopted to describe the equilibrium adsorption. The adsorption data in this study were fitted by the Langmuir model (Eq. 12) and Freundlich model (Eq. 13), respectively (Baskaralingam *et al.* 2006),

$$\frac{C_e}{Q_e} = \frac{1}{k_L \times Q_m} + \frac{C_e}{Q_m} \quad (12)$$

$$\mathrm{Log}Q_e = \mathrm{Log}K_F + \frac{1}{n} \times \mathrm{Log}C_e \quad (13)$$

where C_e (mg/g) is the equilibrium concentration of MB; Q_m (mg/g) is the maximum monolayer adsorption capacity; k_L and K_F are the Langmuir constant and the Freundlich constant, respectively; and n (L/mg) is the Freundlich parameter.

The parameters calculated by two models are given in Table 3. The value of the coefficients of determination (R^2) show that the Langmuir model describes the adsorption behavior of MB onto the hydrogels better. The result suggests a homogeneous surface for each hydrogel and a monolayer adsorption of MB on each hydrogel. The magnitude of the

adsorption intensity *n* gives an indication of the favorability of the adsorbent/adsorbate system. The *n* values indicate beneficial adsorption (Baskaralingam *et al.* 2006).

Table 3. Langmuir and Freundlich Parameters for the Adsorption of MB onto Hydrogels with Various Contents of NaLS

Sample code	Langmuir isotherm parameters			Freundlich isotherm parameters		
	Q_m (mg/g)	K_L	R_L^2	K_F ($mg^{1-1/n}L^{1/n}g^{-1}$)	n	R_F^2
Gel-1	2377	0.00469	0.969	54.36	1.887	0.956
Gel-2	2489	0.00507	0.992	45.38	1.730	0.943
Gel-3	2691	0.00398	0.986	39.94	1.675	0.960
Gel-4	2474	0.00330	0.970	37.28	1.724	0.952

Reusability of Hydrogels

The adsorption capacity versus recycle times of the hydrogel is shown in Fig. 8.

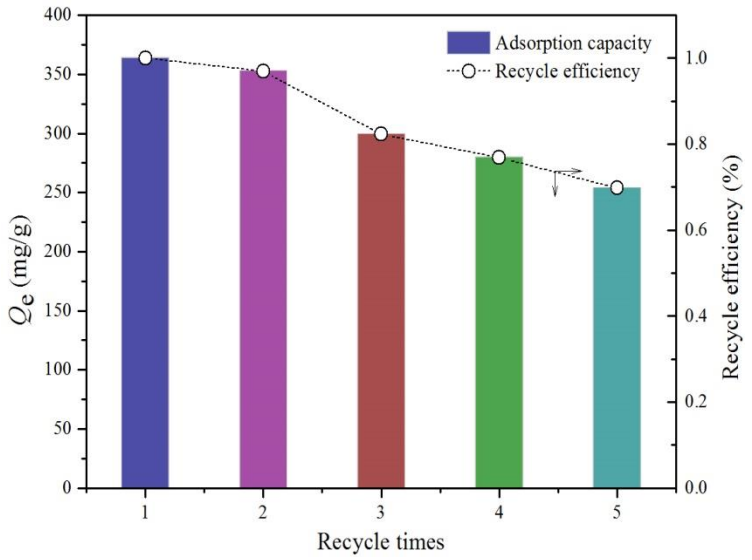

Fig. 8. The reusability of the hydrogel for MB adsorption

It was found that the hydrogel achieved good adsorption capacity and recycle efficiency in the first two recycle times. Afterwards, the adsorption capacity and recycle efficiency decreased during the third to fifth adsorption–desorption cycle. These results may be attributed to the fact that not all the MB molecules adsorbed previously onto the adsorbent have been desorbed during desorption process by HNO_3 solution (a blue hydrogel was seen even after desorption process) (Khan and Lo 2016). Nevertheless, the recycle efficiency was about 80% even after 4 recycle times, which revealed a good reusability of the hydrogel for MB removal.

CONCLUSIONS

1. A porous honeycomb-like hydrogel was prepared by acylated hemicellulose and acrylic acid in the presence of sodium lignosulfonate.

2. An appropriate amount of sodium lignosulfonate into the hydrogel is beneficial for the swelling ratio in deionized water and the adsorption capacity for methylene blue.
3. The hydrogel can be regenerated and reused, and shows about 80% recycle efficiency after 4 recycles.

ACKNOWLEDGMENTS

This work was financially supported by the Key Laboratory of Green Biomass Fuel and Chemicals in Jiangsu Province (Grant Number JSBGFC12006).

REFERENCES CITED

Baskaralingam, P., Pulikesi, M., Elango, D., Ramamurthi, V., and Sivanesan, S. (2006). "Adsorption of acid dye onto organobentonite," *Journal of Hazardous Materials* 128(2-3), 138-144. DOI: 10.1016/j.jhazmat.2005.07.049

Belmokaddem, F. Z., Pinel, C., Huber, P., Petit-Conil, M., and Perez, D. D. (2011). "Green synthesis of xylan hemicellulose esters," *Carbohydrate Research* 346(18), 2896-2904. DOI: 10.1016/j.carres.2011.10.012

Dax, D., Bastidas, M. S. C., Honorato, C., Liu, J., Spoljaric, S., Seppala, J., Mendonca, R. T., Xu, C. L., Willfor, S., and Sanchez, J. (2015). "Tailor-made hemicellulose-based hydrogels reinforced with nanofibrillated cellulose," *Nordic Pulp & Paper Research Journal* 30(3), 373-384. DOI: 10.3183/NPPRJ-2015-30-03-p373-384

Dax, D., Chavez, M. S., Xu, C. L., Willfor, S., Mendonca, R. T., and Sanchez, J. (2014). "Cationic hemicellulose-based hydrogels for arsenic and chromium removal from aqueous solutions," *Carbohydrate Polymers* 111, 797-805. DOI: 10.1016/j.carbpol.2014.05.045

Feng, Q. H., Chen, F. G., and Zhou, X. S. (2012). "Preparation of thermo-sensitive hydrogels from acrylated lignin and n-isopropylacrylamide through photocrosslinking," *Journal of Biobased Materials And Bioenergy* 6(3), 336-342. DOI: 10.1166/jbmb.2012.1218

Feng, Q. H., Li, J. L., Cheng, H. L., Chen, F. G., and Xie, Y. M. (2014). "Synthesis and characterization of porous hydrogel based on lignin and polyacrylamide," *BioResources* 9(3), 4369-4381. DOI: 10.15376/biores.9.3.4369-4381

Fundador, N. G. V., Enomoto-Rogers, Y., Takemura, A., and Iwata, T. (2012). "Syntheses and characterization of xylan esters," *Polymer* 53(18), 3885-3893. DOI: 10.1016/j.polymer.2012.06.038

Goel, N. K., Kumar, V., Misra, N., and Varshney, L. (2015). "Cellulose based cationic adsorbent fabricated via radiation grafting process for treatment of dyes waste water," *Carbohydrate Polymers* 132, 444-451. DOI:10.1016/j.carbpol.2015.06.054

Guo, H. Y., Jiao, T. F., Zhang, Q. R., Guo, W. F., Peng, Q. M., and Yan, X. H. (2015). "Preparation of graphene oxide-based hydrogels as efficient dye adsorbents for wastewater treatment," *Nanoscale Research Letters* 10. DOI: 10.1186/S11671-015-0931-2

Gupta, V. K., Mittal, A., Gajbe, V., and Mittal, J. (2006). "Removal and recovery of the hazardous azo dye acid orange 7 through adsorption over waste materials: Bottom ash

and de-oiled soya," *Industrial & Engineering Chemistry Research* 45(4), 1446-1453. DOI: 10.1021/Ie051111f

Hamcerencu, M., Desbrieres, J., Khoukh, A., Popa, M., and Riess, G. (2008). "Synthesis and characterization of new unsaturated esters of gellan gum," *Carbohydrate Polymers* 71(1), 92-100. DOI: 10.1016/j.carbpol.2007.05.021

Jing, Z. X., Sun, X. F., Ye, Q., and Li, Y. J. (2012). "Hemicellulose-based porous hydrogel for methylene blue adsorption," *Material Sciences and Technology, Pts 1 & 2*, 560-561, 482-487. DOI: 10.4028/www.scientific.net/AMR.560-561.482

Kannan, N., and Sundaram, M. M. (2001). "Kinetics and mechanism of removal of methylene blue by adsorption on various carbons - A comparative study," *Dyes And Pigments*, 51(1), 25-40. DOI: 10.1016/S0143-7208(01)00056-0

Khan, M., and Lo, I. M. (2016). "Removal of ionizable aromatic pollutants from contaminated water using nano γ-Fe_2O_3 based magnetic cationic hydrogel: Sorptive performance, magnetic separation and reusability," *Journal of Hazardous Materials*. DOI: 10.1016/j.jhazmat.2016.01.051

Kumar, R., Singh R., Kumar, N., Bishnoi, K., and Bishnoi, N. R. (2009). "Response surface methodology approach for optimization of biosorption process for removal of Cr (VI), Ni (II) and Zn (II) ions by immobilized bacterial biomass sp. *Bacillus brevis*," *Chemical Engineering Journal* 146, 401–407 DOI: 10.1016/j.cej.2008.06.020

Liu, Y., Wang, W. B., Jin, Y. L., and Wang, A. Q. (2011). "Adsorption behavior of methylene blue from aqueous solution by the hydrogel composites based on attapulgite," *Separation Science and Technology* 46(5), 858-868. DOI: 10.1080/01496395.2010.528502

Mahdavinia, G. R., Pourjavadi, A., Hosseinzadeh, H., and Zohuriaan, M. J. (2004). "Modified chitosan 4. Superabsorbent hydrogels from poly(acrylic acid-co-acrylamide) grafted chitosan with salt- and pH-responsiveness properties," *European Polymer Journal* 40(7), 1399-1407. DOI: 10.1016/j.europolymj.2004.01.039

Mekewi, M. A., Madkour, T. M., Darwish, A. S., and Hashish, Y. M. (2015). "Does poly(acrylic acid-co-acrylamide) hydrogel be the pluperfect choiceness in treatment of dyeing wastewater? From simple copolymer to gigantic aqua-waste remover," *Journal of Industrial and Engineering Chemistry* 30, 359-371. DOI: 10.1016/j.jiec.2015.05.040

Ouyang, X. P., Qiu, X. Q., Lou, H. M., and Yang, D. J. (2006). "Corrosion and scale inhibition properties of sodium lignosulfonate and its potential application in recirculating cooling water system," *Industrial & Engineering Chemistry Research* 45(16), 5716-5721. DOI: 10.1021/Ie0513189

Peng, Q., Liu, M. X., Zheng, J. W., and Zhou, C. R. (2015). "Adsorption of dyes in aqueous solutions by chitosan-halloysite nanotubes composite hydrogel beads," *Microporous and Mesoporous Materials* 201, 190-201. DOI: 10.1016/j.micromeso.2014.09.003

Peng, X. W., Zhong, L. X., Ren, J. L., and Sun, R. C. (2012). "Highly effective adsorption of heavy metal ions from aqueous solutions by macroporous xylan-rich hemicelluloses-based hydrogel," *Journal of Agricultural and Food Chemistry* 60(15), 3909-3916. DOI: 10.1021/Jf300387q

Uraki, Y., Imura, T., Kishimoto, T., and Ubukata, M. (2004). "Body temperature-responsive gels derived from hydroxypropylcellulose bearing lignin," *Carbohydrate Polymers* 58(2), 123-130. DOI: 10.1016/j.carbpol.2004.05.019

Yang, J. Y., Zhou, X. S., and Fang, J. (2011). "Synthesis and characterization of temperature sensitive hemicellulose-based hydrogels," *Carbohydrate Polymers* 86(3), 1113-1117. DOI: 10.1016/j.carbpol.2011.05.043

Yi, J. Z., and Zhang, L. M. (2008). "Removal of methylene blue dye from aqueous solution by adsorption onto sodium humate/polyacrylamide/clay hybrid hydrogels," *Bioresource Technology* 99(7), 2182-2186. DOI: 10.1016/j.biortech.2007.05.028

Zhao, S. P., Zhou, F., Li, L. Y., Cao, M. J., Zuo, D. Y., and Liu, H. T. (2012). "Removal of anionic dyes from aqueous solutions by adsorption of chitosan-based semi-IPN hydrogel composites," *Composites Part B-Engineering* 43(3), 1570-1578. DOI: 10.1016/j.compositesb.2012.01.015

Article submitted: September 3, 2015; Peer review completed: October 16, 2015; Revised version received and accepted: May 10, 2016; Published: June 13, 2016.
DOI: 10.15376/biores.11.3.6378-6392